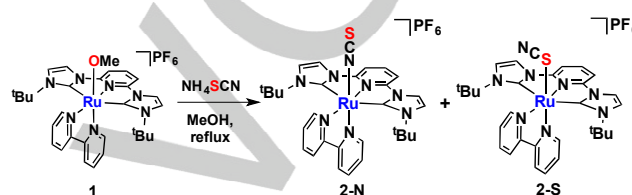


Reactivity of a Methoxido Ruthenium Complex bearing a Pincer-type Bis(carbene) Ligand toward Thiocyanate, Carbon disulfide, and Isothiocyanate

Yasuhiro Arikawa,^{*[a]} Takuo Nakamura,^[a] Takefumi Higashi,^[a] Shinnosuke Horiuchi,^[a] Eri Sakuda,^[a] and Keisuke Umakoshi^[a]

Abstract: Thiocyanate linkage isomers and two insertion complexes were prepared from a methoxido ruthenium complex bearing a 2,6-bis(3-*tert*-butylimidazol-2-ylidene)pyridine (CNC) and a bipyridine ligands. In the linkage isomers obtained from the substitution reaction, a linear N-bound and a bent S-bound isomers were crystallographically determined, and the equilibrium between them at elevated temperature was revealed. On the other hand, in the reactions with carbon disulfide CS₂ and phenyl isothiocyanate PhNCS, the S=C bond was inserted into the Ru–OMe bond, and the resulting ligands are bound to the ruthenium by sulfur.



Scheme 1. Substitution reaction of 1 with NH₄SCN.

Introduction

Recently, researchers have shown an increased interest in pincer complexes which consist of a pincer-type ligand and a metal center.^[1] Of the pincer-type ligand, NHC (*N*-heterocyclic carbene)^[2] has received considerable attention because of its superior σ -donation. We have reported preparations and reactivity of pyridine-based bis(carbene) complexes (CNC complexes),^[3] including interesting capture of CO₂ from air by ruthenium complexes.^[3a] In this fixation of atmospheric carbon dioxide, intermediacy of a methoxido complex [(CNC)Ru(bpy)(OMe)]PF₆ (**1**) was revealed. The observation of the reactive methoxido complex motivated us to investigate its reactivity, in particular, toward sulfur-containing reagents (ammonium thiocyanate NH₄SCN, carbon disulfide CS₂, and phenyl isothiocyanate PhNCS). To the best of our knowledge, interactions between the CNC complexes and sulfur-containing reagents have little explored. This research would provide a fundamental understanding of mechanism in catalytic reaction such as organotransformation reactions.

Results and Discussion

The reaction of [(CNC)Ru(bpy)(OMe)]PF₆ (**1**) with NH₄SCN in refluxing methanol for 2h afforded a mixture of two compounds (ca. 1:1 ratio) as determined by ¹H NMR spectrum (Scheme 1).

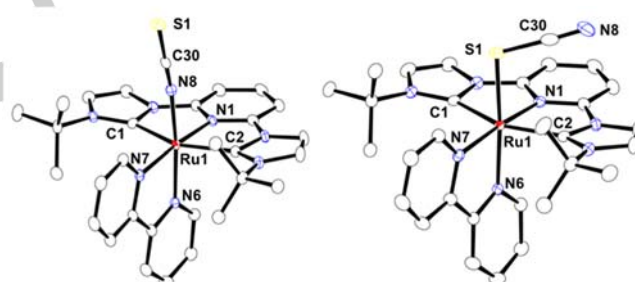


Figure 1. Molecular structures of the cation parts in **2-N** (left) and **2-S** (right). Thermal ellipsoids are set at the 50% probability level. Hydrogen atoms are omitted for clarity. Selected bond lengths [Å] and angles [°] are as follows. For **2-N**: Ru(1)–C(1) 2.128(2), Ru(1)–C(2) 2.124(2), Ru(1)–N(1) 2.013(2), Ru(1)–N(6) 2.055(2), Ru(1)–N(7) 2.074(2), Ru(1)–N(8) 2.043(2), S(1)–C(30) 1.642(3), N(8)–C(30) 1.160(4); Ru(1)–N(8)–C(30) 168.94(19), S(1)–C(30)–N(8) 178.5(2). For **2-S**: Ru(1)–C(1) 2.128(3), Ru(1)–C(2) 2.128(3), Ru(1)–S(1) 2.4248(6), Ru(1)–N(1) 2.007(3), Ru(1)–N(6) 2.0599(16), Ru(1)–N(7) 2.081(3), S(1)–C(30) 1.681(2), N(8)–C(30) 1.162(3); Ru(1)–S(1)–C(30) 104.76(8), S(1)–C(30)–N(8) 177.2(3).

Separation of these two compounds was successful by column chromatography with a silica gel. The ESI-MS spectra of the two compounds show the same signals at m/z 639.29 ([M–PF₆]⁺), indicating linkage isomers. These compounds were also prepared from the reaction between a chlorido complex [(CNC)Ru(bpy)Cl]PF₆ and NH₄SCN. Finally, these structures were confirmed by the X-ray crystallographic analysis.

The column chromatographic purification afforded [(CNC)Ru(bpy)(NCS)]PF₆ (**2-N**) from the first band and [(CNC)Ru(bpy)(SCN)]PF₆ (**2-S**) from the second band. The X-ray crystal structures of **2** are shown in Figure 1. In both structures, the meridional CNC and bipyridine ligands are bound to the Ru atom, and the distorted octahedral geometry is completed by the thiocyanato ligand. As a distinct difference, a linear NCS form in

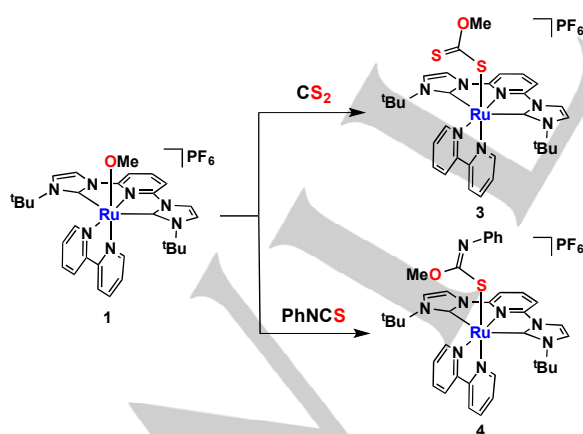
[a] Division of Chemistry and Materials Science, Graduate School of Engineering, Nagasaki University, Bunkyo-machi 1-14, Nagasaki 852-8521, Japan.
E-mail: arikawa@nagasaki-u.ac.jp

Supporting information for this article is given via a link at the end of the document.

FULL PAPER

2-N ($\text{Ru}(1)\text{--N}(8)\text{--C}(30) = 168.94(19)^\circ$) and a bent SCN form in **2-S** ($\text{Ru}(1)\text{--S}(1)\text{--C}(30) = 104.76(8)^\circ$) are observed. The Ru–NCS distance ($\text{Ru}(1)\text{--N}(8)$, 2.043(2) Å) in **2-N** and the Ru–SCN distance ($\text{Ru}(1)\text{--S}(1)$, 2.4248(6) Å) in **2-S** are similar to those in the corresponding isomers of $[(p\text{-cymene})\text{Ru}(\text{bpy})(\text{thiocyanato})]\text{PF}_6$ ^[4] and $[(\text{terpy})\text{Ru}(\text{tbbpy})(\text{thiocyanato})]\text{SbF}_6$ ^[5] (terpy = 2,2',6',2"-terpyridine, tbbpy = 4,4'-di-tert-butyl-2,2'-bipyridine), where both linkage isomers have been crystallographically determined. There is little difference in the structure of the thiocyanato moiety in **2-N** and **2-S** ($\text{N}(8)\text{--C}(30) = 1.160(4)$ (**2-N**), 1.162(3) Å (**2-S**); $\text{S}(1)\text{--C}(30) = 1.642(3)$ (**2-N**), 1.681(2) Å (**2-S**); $\text{S}(1)\text{--C}(30)\text{--N}(8) = 178.5(2)$ (**2-N**), 177.2(3)° (**2-S**)). The ¹H NMR spectroscopy revealed that heating of a dms_o-d₆ solution of **2-N** at 120°C for 2h gave a mixture of **2-N** and **2-S** at ca. 1:0.13 ratio, though the isomerisation did not proceed at room temperature. Longer heating did not affect the ratio of the two isomers. These results indicate the existence of equilibrium in the mixture. The **2-S** isomer is thermodynamically unfavorable, which is the same trend as $[(\text{terpy})\text{Ru}(\text{tbbpy})(\text{thiocyanate})]\text{SbF}_6$ ^[5]. The steric hindrance between a bent SCN ligand and two ^tBu moiety on the CNC ligand would be attributed to the lower stability of **2-S** isomer.

On the other hand, in the reaction with CS₂ and PhNCS, insertion reactions were observed (Scheme 2). Treatment of $[(\text{CNC})\text{Ru}(\text{bpy})(\text{OMe})]\text{PF}_6$ (**1**) with CS₂ and PhNCS gave rise to $[(\text{CNC})\text{Ru}(\text{bpy})\{\text{SC}(\text{S})\text{OMe}\}]\text{PF}_6$ (**3**) and $[(\text{CNC})\text{Ru}(\text{bpy})\{\text{SC}(\text{NPh})\text{OMe}\}]\text{PF}_6$ (**4**), respectively. A $\nu(\text{C}=\text{S})$ stretching band at 1620 cm⁻¹ is observed in the IR spectrum of **3**. The ESI-MS spectra of **3** and **4** exhibit the molecular ion signals at m/z 688.1(**3**) and m/z 747.3 (**4**), which show CS₂ and PhNCS mass increments, respectively, as compared to $[(\text{CNC})\text{Ru}(\text{bpy})(\text{OMe})]^+$, indicating their incorporation. Although reaction of **1** with ^tBuNCS proceeded, isolation of the products was unsuccessful. The molecular structures of **3** and **4** were determined by the X-ray crystallographic analyses (Figure 2 and 3).



Scheme 2. Insertion reactions of **1** with CS₂ and PhNCS.

The κ^1 -coordinated xanthato ligand in **3** and monodentate sulfur-coordination in **4** are revealed, along with coordination of the CNC and bpy ligands to the Ru atom. The sulfur-coordination

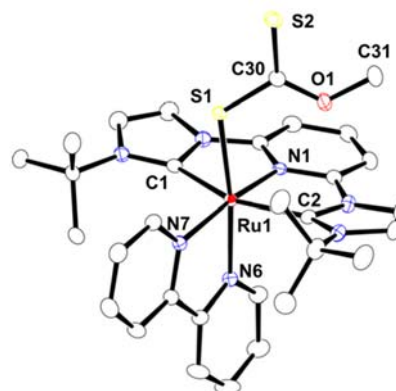


Figure 2. Molecular structure of the cation part in **3** with thermal ellipsoids drawn at the 50% probability level. Hydrogen atoms are omitted for clarity. Selected bond lengths [Å] and angles [°]: $\text{Ru}(1)\text{--C}(1)$ 2.1278(19), $\text{Ru}(1)\text{--C}(2)$ 2.1026(19), $\text{Ru}(1)\text{--S}(1)$ 2.3776(7), $\text{Ru}(1)\text{--N}(1)$ 2.0021(15), $\text{Ru}(1)\text{--N}(6)$ 2.0814(17), $\text{Ru}(1)\text{--N}(7)$ 2.0879(15), $\text{S}(1)\text{--C}(30)$ 1.7148(16), $\text{S}(2)\text{--C}(30)$ 1.6694(19), $\text{O}(1)\text{--C}(30)$ 1.338(3); $\text{Ru}(1)\text{--S}(1)\text{--C}(30)$ 117.95(8), $\text{S}(1)\text{--C}(30)\text{--S}(2)$ 121.34(12), $\text{S}(1)\text{--C}(30)\text{--O}(1)$ 115.19(13), $\text{S}(2)\text{--C}(30)\text{--O}(1)$ 123.46(12).

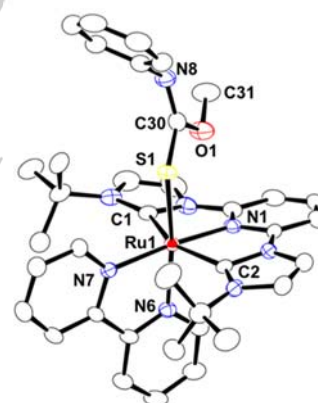


Figure 3. Molecular structure of the cation part in **4** with thermal ellipsoids drawn at the 50% probability level. Hydrogen atoms are omitted for clarity. Selected bond lengths [Å] and angles [°]: $\text{Ru}(1)\text{--C}(1)$ 2.127(4), $\text{Ru}(1)\text{--C}(2)$ 2.135(4), $\text{Ru}(1)\text{--S}(1)$ 2.4279(11), $\text{Ru}(1)\text{--N}(1)$ 2.010(3), $\text{Ru}(1)\text{--N}(6)$ 2.067(3), $\text{Ru}(1)\text{--N}(7)$ 2.081(3), $\text{S}(1)\text{--C}(30)$ 1.741(4), $\text{O}(1)\text{--C}(30)$ 1.357(5), $\text{N}(8)\text{--C}(30)$ 1.285(5); $\text{Ru}(1)\text{--S}(1)\text{--C}(30)$ 112.78(15), $\text{S}(1)\text{--C}(30)\text{--O}(1)$ 112.6(3), $\text{S}(1)\text{--C}(30)\text{--N}(8)$ 130.0(3), $\text{O}(1)\text{--C}(30)\text{--N}(8)$ 117.4(4).

in **4** indicates that the S=C bond rather than N=C was inserted into the ruthenium–methoxido bond. Similar insertion reactions have been observed in other alkoxido-metal complexes,^[6] probably due to the HSAB principle, with the soft ruthenium center preferring the softer sulfur atom. The Ru–S bond length of **3** (2.3776(7) Å) is shorter than that of **4** (2.4279(11) Å). The former is similar to that of a monodentate xanthato ruthenium complex $\text{trans}[\text{Ru}(\text{CO})(\text{PEt}_3)_2(\eta^1\text{-S}_2\text{COEt})(\eta^2\text{-S}_2\text{COEt})]$ (2.3915(8) Å).^[7] The S–C distances for the coordinated and uncoordinated sulfur atoms of the xanthato ligand of **3** (1.7148(16) and 1.6694(19) Å, respectively) are almost identical to the distances found in $\text{trans}[\text{Ru}(\text{CO})(\text{PEt}_3)_2(\eta^1\text{-S}_2\text{COEt})(\eta^2\text{-S}_2\text{COEt})]$,^[7] $[\text{Re}\{\text{SC}(\text{S})\text{OCH}_3\}(\text{CO})_3(\text{bpy})]$,^[6a] $[(\text{C}_5\text{R}_5)\text{Fe}(\text{CO})_2\{\text{SC}(\text{S})\text{OEt}\}]$ (R = H, Me),^[8] and $[\text{W}(\eta^1\text{-S}_2\text{COPr})(\eta^2\text{-S}_2\text{COPr})(\text{CO})_2(\text{PMe}_3)_2]$.^[9] In

complex **4**, the bond distances S(1)–C(30) (1.741(4) Å) and N(8)–C(30) (1.285(5) Å) are consistent with single and double bonds, respectively. The planarity of the sulfur-coordinated ligands in **3** and **4** is supported by the sum of angles (360°) around the C(30). The insertion reactions giving **3** and **4** should proceed via a four-membered ring transition state without requirement of a binding site for the substrate prior to insertion.^[10] In sharp contrast to this, the formation mechanism of a xanthato complex [TPRu(PPh₃)(κ²-S₂COCH₃)] is a MeOH attack on a coordinated CS₂ ligand.^[11]

Conclusions

We reported reactivity of the methoxido ruthenium complex having the pyridine-based bis(*N-tert*-butyl substituted *N*-heterocyclic carbene) (CNC) and a bipyridine toward the sulfur-containing heteroallenes. In the reaction with NH₄SCN, thiocyanate linkage isomers from the substitution reaction have obtained, structures of which (linear NCS and bent SCN) were determined by the X-ray crystallographic analyses. In contrast, treatment with CS₂ and PhNCS resulted in the formation of SC(=S)OMe and SC(=NPh)OMe groups, respectively, due to insertion of the S=C bond into the Ru–OMe bond. Surprisingly, to the best of our knowledge, the latter is the first reported example of insertion of isothiocyanate into ruthenium–alkoxido bond.

Experimental Section

Materials and General Procedures: All reactions were carried out under N₂ or Ar unless otherwise noted, and subsequent work-up manipulations were performed in air. The starting complex [(CNC)Ru(bpy)(OMe)]PF₆ (**1**) was prepared according to the previously reported method.^[3a] Organic solvents and all other reagents were commercially available and used without further purification. NMR spectra in acetone-d₆ were recorded on a Varian Gemini-300 and a JEOL JNM-AL-400 spectrometers. ¹H and ¹³C{¹H} NMR chemical shifts are quoted with respect to the solvent signals. Infrared spectra in KBr pellets were obtained on JASCO FT-IR-4100 spectrometer. Electrospray mass spectroscopies (ESI-MS) were carried out on a Waters ACQUITY SQD MS system. Elemental analyses (C, H, N) were performed on a Perkin Elmer 2400II elemental analyzer.

Reactions of [(CNC)Ru(bpy)(OMe)]PF₆ (1**) with NH₄SCN.** A mixture of [(CNC)Ru(bpy)(OMe)]PF₆ (**1**) (15 mg, 0.02 mmol) and NH₄SCN (7.8 mg, 0.10 mmol) in MeOH (5.0 mL) was refluxed for 2 h. After evaporation to dryness, the residue was column-chromatographed with a silica gel eluting with CH₂Cl₂-MeOH (50/1). [(CNC)Ru(bpy)(NCS)]PF₆ (**2-N**) (4.9 mg, 31%) and [(CNC)Ru(bpy)(SCN)]PF₆ (**2-S**) (5.8 mg, 37%) were obtained. **2-N:** IR (KBr, pellet): ν(CN) 2118 (s) cm⁻¹, ν(PF) 849 (s) cm⁻¹. ¹H NMR (acetone-d₆): δ 9.63 (d, *J* = 5.5 Hz, 1H, bpy), 8.76 (d, *J* = 7.9 Hz, 1H, bpy), 8.56 (d, *J* = 7.9 Hz, 1H, bpy), 8.38 (d, *J* = 2.3 Hz, 2H, imid), 8.26–8.35 (m, 2H, bpy + 4-py), 8.14 (d, *J* = 8.1 Hz, 2H, 3,5-py), 8.10 (m, 1H, bpy), 7.81 (m, 1H, bpy), 7.60 (d, *J* = 2.4 Hz, 2H, imid), 7.37 (d, *J* = 5.5 Hz, 1H, bpy), 7.12 (m, 1H, bpy), 1.12 (s, 18H, 'Bu). ¹³C{¹H} NMR (acetone-d₆): δ 189.4 (Ru-C_{NHC}), 158.4 (NCS), 158.1 (bpy), 155.2 (bpy), 155.0 (2,6-py), 151.7 (bpy), 140.5 (4-py), 136.7 (bpy), 135.9 (bpy), 126.9 (bpy), 126.9 (bpy), 124.3 (bpy), 123.9 (bpy), 122.6 (imid), 116.9 (imid), 107.5 (3,5-py), 58.7 (CCH₃), 31.1 (CCH₃). Signal of one bpy carbon was not determined, probably because of accidental overlapping with other signals. ESI-MS (*m/z*): 639.29 [M-PF₆]⁺. Elemental analysis (%) calcd for C₃₀H₃₃N₈SRuPF₆: C, 45.97; H, 4.24; N, 14.30; found: C, 45.95; H, 4.59; N, 14.22. **2-S:** IR (KBr, pellet): ν(CN) 2099 (s) cm⁻¹, ν(PF) 846 (s) cm⁻¹. ¹H NMR (acetone-d₆): δ 10.00

(*J* = 5.8 Hz, 1H, bpy), 8.76 (d, *J* = 7.9 Hz, 1H, bpy), 8.56 (d, *J* = 7.9 Hz, 1H, bpy), 8.38 (d, *J* = 2.4 Hz, 2H, imid), 8.23–8.34 (m, 2H, bpy + 4-py), 8.13 (d, *J* = 7.9 Hz, 2H, 3,5-py), 8.00 (m, 1H, bpy), 7.87 (m, 1H, bpy), 7.61 (d, *J* = 5.7 Hz, 1H, bpy), 7.56 (d, *J* = 2.4 Hz, 2H, imid), 7.17 (m, 1H, bpy), 1.14 (s, 18H, 'Bu). ¹³C{¹H} NMR (acetone-d₆): δ 190.0 (Ru-C_{NHC}), 159.0 (SCN), 157.7 (bpy), 155.7 (bpy), 154.8 (2,6-py), 152.0 (bpy), 140.1 (4-py), 136.6 (bpy), 136.3 (bpy), 126.8 (bpy), 126.7 (bpy), 124.3 (bpy), 123.9 (bpy), 122.9 (imid), 117.2 (imid), 107.2 (3,5-py), 58.6 (CCH₃), 31.4 (CCH₃). Signal of one bpy carbon was not determined, probably because of accidental overlapping with other signals. ESI-MS (*m/z*): 639.29 [M-PF₆]⁺. Elemental analysis (%) calcd for C₃₀H₃₃N₈SRuPF₆: C, 45.97; H, 4.24; N, 14.30; found: C, 45.43; H, 4.45; N, 13.66.

[(CNC)Ru(bpy){SC(S)OMe}]PF₆ (3**):** A J. Young NMR tube was charged with [(CNC)Ru(bpy)(OMe)]PF₆ (**1**) (15 mg, 0.02 mmol) in acetone-d₆ (0.6 mL). CS₂ (6.0 μL, 0.10 mmol) was added to the solution. The solution immediately turned from dark brown to red-orange. After 1 h, ¹H NMR analysis revealed full conversion to the product. The solution was dried *in vacuo*, and the resulting solid was crystallized from acetone/ether to give [(CNC)Ru(bpy){SC(S)OMe}]PF₆ (**3**) as red crystals (14 mg, 84%). IR (KBr, pellet): ν(PF) 846 cm⁻¹, ν(C=S) 1620 cm⁻¹. ¹H NMR (acetone-d₆): δ 10.00 (d, *J* = 5.4 Hz, 1H, bpy), 8.71 (d, *J* = 8.2 Hz, 1H, bpy), 8.56 (d, *J* = 8.0 Hz, 1H, bpy), 8.38 (d, *J* = 2.3 Hz, 2H, imid), 8.19–8.26 (m, 2H, bpy + 4-py), 8.08 (d, *J* = 8.2 Hz, 2H, 3,5-py), 7.99 (m, 1H, bpy), 7.85 (m, 1H, bpy), 7.54 (d, *J* = 2.0 Hz, 2H, imid), 7.46 (d, *J* = 5.4 Hz, 1H, bpy), 7.19 (m, 1H, bpy), 3.34 (s, 3H, SC(S)OCH₃), 1.18 (s, 18H, 'Bu). ¹³C{¹H} NMR (acetone-d₆): δ 227.7 (SC(S)OCH₃), 192.0 (Ru-C_{NHC}), 158.8 (bpy), 157.1 (2,6-py), 155.1 (bpy), 150.7 (bpy), 139.4 (4-py), 136.5 (bpy), 136.2 (bpy), 126.8 (bpy), 126.6 (bpy), 124.3 (bpy), 123.7 (bpy), 122.4 (imid), 122.2 (bpy), 116.7 (imid), 106.6 (3,5-py), 59.3 (OCH₃), 58.5 (CCH₃), 31.1 (CCH₃). ESI-MS (*m/z*): 688.1 [M-PF₆]⁺. Elemental analysis (%) calcd for C₃₁H₃₆N₇OS₂RuPF₆·C₄H₁₀O: C, 46.35; H, 5.11; N, 10.81; found: C, 46.32; H, 5.23; N, 10.95.

[(CNC)Ru(bpy){SC(NPh)OMe}]PF₆ (4**):** A J. Young NMR tube was charged with [(CNC)Ru(bpy)(OMe)]PF₆ (**1**) (15 mg, 0.02 mmol) in acetone-d₆ (0.6 mL). PhNCS (12 μL, 0.10 mmol) was added to the solution. The solution immediately turned from dark brown to red-orange. After 1 h, ¹H NMR analysis revealed full conversion to the product. The solution was dried *in vacuo*, and the resulting solid was crystallized from acetone/ether to give [(CNC)Ru(bpy){SC(NPh)OMe}]PF₆ (**4**) as red crystals (16 mg, 90%). IR (KBr, pellet): ν(PF) 846 (s) cm⁻¹. ¹H NMR (acetone-d₆): δ 10.02 (d, *J* = 5.2 Hz, 1H, bpy), 8.66 (d, *J* = 8.3 Hz, 1H, bpy), 8.53 (d, *J* = 8.2 Hz, 1H, bpy), 8.37 (d, *J* = 2.4 Hz, 2H, imid), 8.26–8.20 (m, 1H, 4-py), 8.13 (td, *J* = 7.8, 1.3 Hz, 1H, bpy), 8.07 (d, *J* = 7.9, 2H, 3,5-py), 7.84–7.77 (m, 2H, bpy), 7.51 (d, *J* = 2.4 Hz, 3H, imid + bpy), 7.14 (m, 3H, bpy + *NPh*), 6.84 (t, *J* = 7.4 Hz, 1H, *NPh*), 6.62 (d, *J* = 8.2 Hz, 2H, *NPh*), 3.03 (s, 3H, *OMe*), 1.08 (s, 18H, 'Bu). ¹³C{¹H} NMR (acetone-d₆): δ 192.7 (Ru-C_{NHC}), 170.4 (SC(OMe)*NPh*), 159.1 (bpy), 157.7 (bpy), 155.7 (bpy), 155.1 (2,6-py), 152.7 (*NPh*), 151.2 (bpy), 138.6 (4-py), 136.0 (bpy), 135.8 (bpy), 128.6 (*NPh*), 126.7 (bpy), 126.0 (bpy), 124.0 (bpy), 123.7 (bpy), 123.3 (*NPh*), 122.2 (imid), 121.8 (*NPh*), 116.5 (imid), 106.3 (3,5-py), 58.4 (CCH₃), 54.5 (OCH₃), 31.4 (CCH₃). ESI-MS (*m/z*): 747.3 [M-PF₆]⁺. Elemental analysis (%) calcd for C₃₇H₄₁N₈OSRuPF₆: C, 49.83; H, 4.63; N, 12.56; found: C, 50.09; H, 4.36; N, 12.25.

X-ray Crystallography: Crystallographic data are summarized in Table S1 (Supporting information). X-ray quality single crystals were obtained from MeOH/ether (for **2-N** and **2-S**) and acetone/ether (for **3-ether** and **4-ether**). Diffraction data were collected at -180°C under a stream of cold N₂ gas on a Rigaku RA-Micro7 HFM instrument equipped with a Rigaku Saturn724+ CCD detector by using graphite-monochromated Mo-Kα radiation. The intensity images were obtained at the exposure of 16.0 s/° (**2-N** and **2-S**), 4.0 s/° (**3-ether**), and 8.0 s/° (**4-ether**). The frame data were

FULL PAPER

integrated using a Rigaku CrystalClear program package, and the data sets were corrected for absorption using a REQAB program.

The calculations were performed with a CrystalStructure software package. The structures were solved by direct methods, and refined on F^2 by the full-matrix least squares methods. For **3**-ether and **4**-ether, a diethylether crystallization solvent is included. For **2-S**, owing to serious disorder problems of the crystallization solvents, we were not able to well define them. Therefore, a SQUEEZE/PLATON technique was applied. Anisotropic refinement was applied to all non-hydrogen atoms. Hydrogen atoms for all structures were put at calculated positions.

CCDC 1514524–1514527 (for **2-N**, **2-S**, **3**, and **4**) contain the supplementary crystallographic data for this paper. These data can be obtained free of charge from The Cambridge Crystallographic Data Centre.

Acknowledgements

This work was supported by the priority research project of Nagasaki University.

Keywords: Bis(carbene) ligand • Linkage isomers • Insertion • Methoxide • Ruthenium

- [1] a) C. Gunanathan, D. Milstein, *Chem. Rev.* **2014**, *114*, 12024-12087 and references therein; b) D. Morales-Morales, C. M. Jensen, *The Chemistry of Pincer Compounds*, Elsevier, Amsterdam, **2007**; c) M. Asay, D. Morales-Morales, *Dalton Trans.* **2015**, *44*, 17432-17447; d) S. Murugesan, K. Kirchner, *Dalton Trans.* **2016**, *45*, 416-439; e) G. v. Koten, R. A. Gossage, *The Privileged Pincer-Metal Platform: Coordination Chemistry & Applications*, Vol. 54, Springer, 2016; f) R. E. Andrew, L. Gonzalez-Sebastian, A. B. Chaplin, *Dalton Trans.* **2016**, *45*, 1299-1305.
- [2] a) S. P. Nolan, *N-Heterocyclic Carbenes: Effective Tools for Organometallic Synthesis*, Wiley-VCH, Weinheim, **2014**; b) C. S. J. Cazin, *N-Heterocyclic Carbenes in Transition Metal Catalysis and Organocatalysis*, Springer, Heidelberg, **2011**; c) M. Bierenstiel, E. D. Cross, *Coord. Chem. Rev.* **2011**, *255*, 574-590; d) O. Kühn, *Functionalised N-Heterocyclic Carbene Complexes*, Wiley, Chichester, **2010**; e) T. Dröge, F. Glorius, *Angew. Chem. Int. Ed.* **2010**, *49*, 6940-6952; f) S. Diez-Gonzalez, *N-Heterocyclic Carbenes: From Laboratory Curiosities to Efficient Synthetic Tools*, RSC, Cambridge, **2010**; g) F. E. Hahn, M. C. Jahnke, *Angew. Chem. Int. Ed.* **2008**, *47*, 3122-3172; h) D. Pugh, A. A. Danopoulos, *Coord. Chem. Rev.* **2007**, *251*, 610-641; i) J. A. Mata, M. Poyatos, E. Peris, *Coord. Chem. Rev.* **2007**, *251*, 841-859; j) E. A. B. Kantchev, C. J. O'Brien, M. G. Organ, *Angew. Chem. Int. Ed.* **2007**, *46*, 2768-2813; k) F. Glorius, *N-Heterocyclic Carbenes in Transition Metal Catalysis*, Springer, New York, **2007**; l) S. P. Nolan, *N-Heterocyclic Carbenes in Synthesis*, Wiley, New York, **2006**; m) R. H. Crabtree, *J. Organomet. Chem.* **2005**, *690*, 5451-5457; n) C. M. Crudden, D. P. Allen, *Coord. Chem. Rev.* **2004**, *248*, 2247-2273; o) W. A. Herrmann, *Angew. Chem. Int. Ed.* **2002**, *41*, 1290-1309; p) D. Bourissou, O. Guerret, F. P. Gabbaï, G. Bertrand, *Chem. Rev.* **2000**, *100*, 39-92; q) A. J. Arduengo, *Acc. Chem. Res.* **1999**, *32*, 913-921.
- [3] a) Y. Arikawa, T. Nakamura, S. Ogushi, K. Eguchi, K. Umakoshi, *Dalton Trans.* **2015**, *44*, 5303-5305; b) T. Nakamura, S. Ogushi, Y. Arikawa, K. Umakoshi, *J. Organomet. Chem.* **2016**, *803*, 67-72.
- [4] L. Vandenburg, M. R. Buck, D. A. Freedman, *Inorg. Chem.* **2008**, *47*, 9134-9136.
- [5] T. P. Brewster, W. Ding, N. D. Schley, N. Hazari, V. S. Batista, R. H. Crabtree, *Inorg. Chem.* **2011**, *50*, 11938-11946.
- [6] a) E. Hevia, J. Pérez, L. Riera, V. Riera, I. del Río, S. García-Granda, D. Miguel, *Chem. Eur. J.* **2002**, *8*, 4510-4521; b) J. Cámpora, I. Matas, P. Palma, E. Álvarez, C. Graiff, A. Tiripicchio, *Organometallics* **2007**, *26*, 3840-3849; c) H. Brombacher, H. Vahrenkamp, *Inorg. Chem.* **2004**, *43*, 6042-6049; d) C. Wycliff, A. G. Samuelson, M. Nethaji, *Inorg. Chem.* **1996**, *35*, 5427-5434.
- [7] A. J. Deeming, C. Forth, G. Hogarth, *J. Organomet. Chem.* **2006**, *691*, 79-85.
- [8] M. Morán, I. Cuadrado, J. R. Masaguer, J. Losada, C. Foces-Foces, F. H. Cano, *Inorg. Chim. Acta* **1988**, *143*, 59-70.
- [9] E. Carmona, L. Contreras, L. J. Sanchez, E. Gutierrez-Puebla, A. Monge, *J. Chem. Soc., Dalton Trans.* **1989**, 2003-2009.
- [10] a) R. D. Simpson, R. G. Bergman, *Angew. Chem. Int. Ed. Engl.* **1992**, *31*, 220-223; b) R. D. Simpson, R. G. Bergman, *Organometallics* **1992**, *11*, 4306-4315; c) S. K. Mandal, D. M. Ho, M. Orchin, *Organometallics* **1993**, *12*, 1714-1719; d) D. J. Darensbourg, W.-Z. Lee, A. L. Phelps, E. Guidry, *Organometallics* **2003**, *22*, 5585-5588.
- [11] W.-L. Huang, G.-J. Hung, Y.-H. Lo, *J. Organomet. Chem.* **2014**, *767*, 120-124.



Thiocyanate linkage isomers and two insertion complexes were prepared from a methoxido ruthenium complex bearing a pyridine-based bis(carbene) (CNC) and a bipyridine ligands. In the linkage isomers obtained from the substitution reaction, a linear N-bound and a bent S-bound isomer were crystallographically determined. On the other hand, in the reactions with carbon disulfide CS_2 and phenyl isothiocyanate $PhNCS$, the S=C bond was inserted into the Ru-OMe bond.

Ruthenium CNC Pincer Complexes

Yasuhiro Arikawa,^{*[a]} Takuo Nakamura,^[a] Takefumi Higashi,^[a] Shinnosuke Horiuchi,^[a] Eri Sakuda,^[a] and Keisuke Umakoshi^{†[a]}

Page No. – Page No.

Reactivity of a Methoxido Ruthenium Complex bearing a Pincer-type Bis(carbene) Ligand toward Thiocyanate, Carbon disulfide, and Isothiocyanate